

# Nernst and Ettingshausen Effects in Silicon between 300°K and 800°K

HERBERT METTE, WOLFGANG W. GÄRTNER, AND CLAIRE LOSCOE  
*U. S. Army Signal Research and Development Laboratory, Fort Monmouth, New Jersey*  
 (Received October 13, 1959)

The Nernst and Ettingshausen coefficients in *p*-type silicon single crystals of various impurity densities have been measured over a temperature range between 300°K and 800°K at magnetic fields of 9000 gauss. The results are in good agreement with the theoretical predictions. Using the measured coefficients in the Bridgman relation, values were obtained for the thermal conductivity of silicon in the temperature range between 550°K and 800°K.

## 1. INTRODUCTION

THE recently reported investigation of the high-temperature Nernst and Ettingshausen effects in germanium<sup>1</sup> has been extended to silicon for which, to our knowledge, no such measurements have been reported previously. The experimental arrangement and the theoretical expressions used were essentially the same as in reference 1, and the interested reader is referred to this paper for details of the measuring apparatus and of the assumptions underlying the theory.

## 2. THEORETICAL PREDICTIONS

Figures 1(a) and 1(b) show the theoretical Nernst coefficient,  $B$ , in *n*- and *p*-type silicon as a function of temperature for various impurity densities. The curves

were calculated from the expression

$$B = [qD(\mu_n^H + \mu_p^H)/\sigma(n_0 + p_0)]d(n_i^2)/dT, \quad (1)$$

where  $q$  is the electronic charge;  $D$  is the ambipolar diffusivity;  $\sigma$  is the conductivity,  $\sigma = q(\mu_n^D n_0 + \mu_p^D p_0)$ ;  $n_0$  and  $p_0$  are the equilibrium carrier densities;  $T$  is the absolute temperature;  $n_i$  is the intrinsic carrier density;  $\mu_n^H$  and  $\mu_p^H$  are the electron and hole Hall mobilities;  $\mu_n^D$  and  $\mu_p^D$  are the electron and hole drift mobilities. The following numerical values were used<sup>2-4</sup>:

$$n_i^2 = 1.5 \times 10^{33} \times T^3 \times \exp(-14\,028/T),$$

$$\mu_n^D = (2.1 \pm 0.2) \times 10^9 \times T^{-2.5 \pm 0.1} \text{ cm}^2 \text{ v}^{-1} \text{ sec}^{-1},$$

$$\mu_n^H = 1.52 \mu_n^D,$$

$$\mu_p^D = (2.3 \pm 0.1) \times 10^9 \times T^{-2.7 \pm 0.1} \text{ cm}^2 \text{ v}^{-1} \text{ sec}^{-1},$$

$$\mu_p^H = 0.885 \mu_p^D.$$

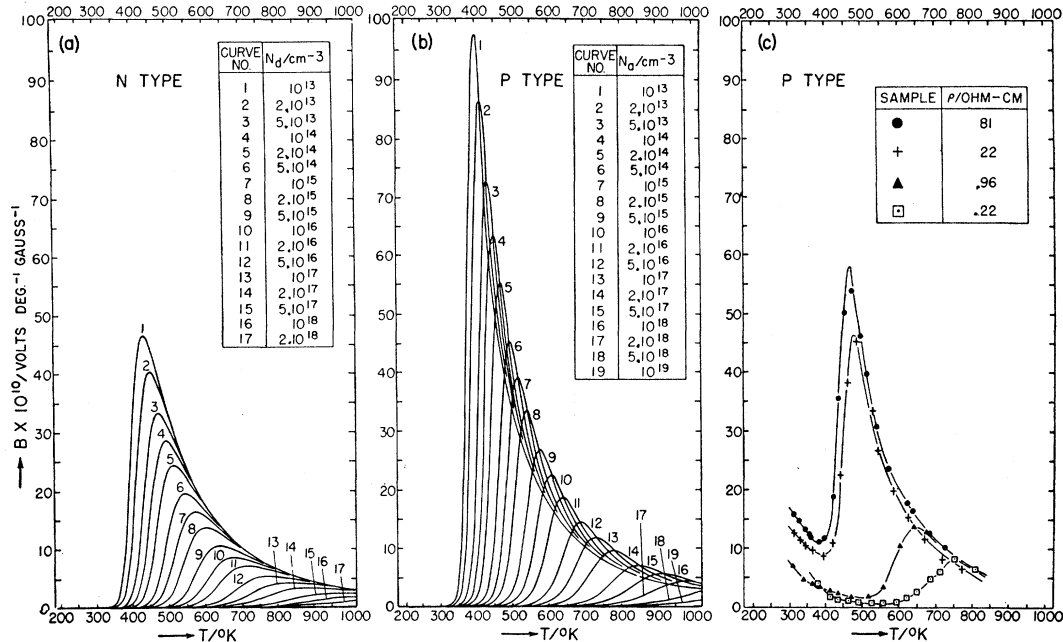


FIG. 1. Nernst coefficient,  $B$ , in silicon with various impurity concentrations as a function of temperature; (a) theoretical for *n*-type; (b) theoretical for *p*-type; (c) experimental for *p*-type at 9000 gauss.

<sup>1</sup> H. Mette, W. W. Gärtner, and C. Loscoe, Phys. Rev. **115**, 537 (1959).

<sup>2</sup> F. J. Morin and J. P. Maita, Phys. Rev. **96**, 28 (1954).

<sup>3</sup> G. W. Ludwig and R. L. Watters, Phys. Rev. **101**, 1699 (1956).

<sup>4</sup> P. P. Debye and T. Kohane, Phys. Rev. **95**, 724 (1954).

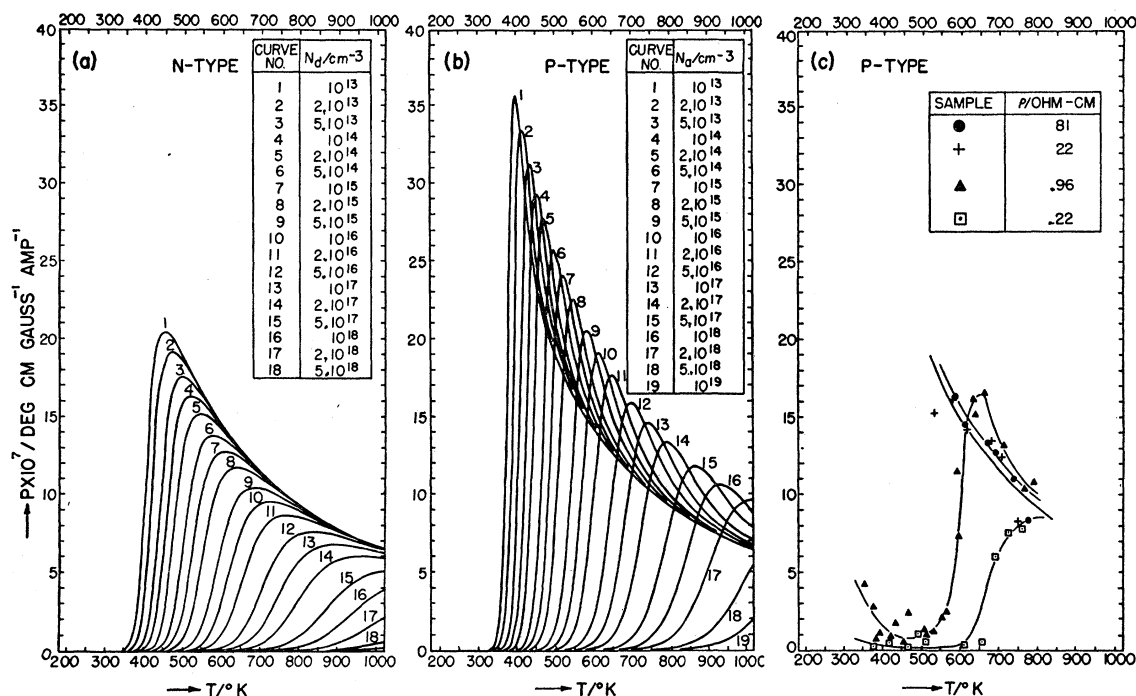


FIG. 2. Ettingshausen coefficient,  $P$ , in silicon with various impurity concentrations as a function of temperature; (a) theoretical for  $n$ -type; (b) theoretical for  $p$ -type; (c) experimental for  $p$ -type at 9000 gauss.

Theoretical values for the Ettingshausen coefficient,  $P$ , were obtained by means of the Bridgman relation,  $BT = \kappa P$ , where the thermal conductivity,  $\kappa$ , was approximated by the expression

$$\kappa = 435/T \text{ watts deg}^{-1} \text{ cm}^{-1}, \quad (2)$$

which is an extrapolation towards higher temperatures of the room-temperature value reported by Carruthers

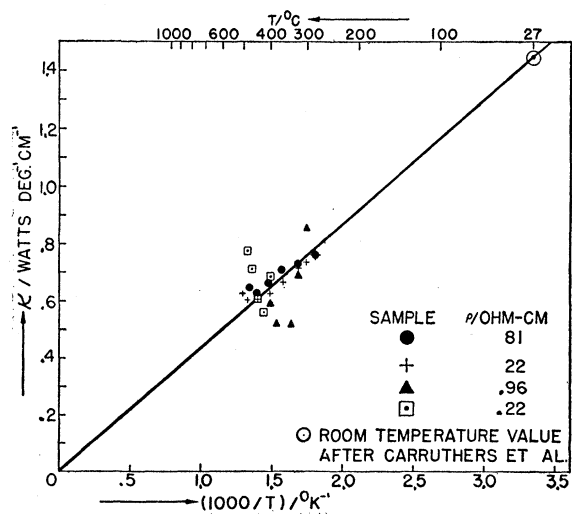


FIG. 3. Heat conductivity of silicon calculated from the Nernst and Ettingshausen coefficients.

*et al.*<sup>5</sup> These theoretical values were plotted in Figs. 2(a) and 2(b) as a function of temperature for various impurity densities.

### 3. EXPERIMENTS

The measuring procedure for both effects in silicon was essentially the same as that for germanium.<sup>1</sup> Good ohmic contacts to the  $p$ -type material were obtained by rhodium plating. Since the effects are considerably smaller in silicon than in germanium, the measurements were normally taken at magnetic fields of 9000 gauss to achieve a sufficiently large reading accuracy. Control measurements at the peak points of the coefficient versus temperature curves, however, showed no dependence of the Nernst or Ettingshausen constants on the magnetic field within the experimental accuracy of several percent.

Figure 1(c) shows the experimental Nernst coefficient for four  $p$ -type silicon samples of various resistivities. The curves are in good agreement with the theoretical curves except at the low-temperature end where the assumptions underlying the theory are not expected to hold.

Figure 2(c) gives the experimental results for the Ettingshausen coefficient obtained for the same samples that were used in the Nernst measurements of Fig. 1(c). Again the agreement between theory and experiment is quite good. Because of the internal heating of the two

<sup>5</sup> J. A. Carruthers, T. H. Geballe, H. M. Rosenberg, and J. M. Ziman, Proc. Roy. Soc. (London) **A238**, 502 (1957).

high-resistivity samples at temperatures below 550°K, data could not be taken with the current densities needed for accurate readings. Therefore, the Ettingshausen coefficient for these high-resistivity samples is reported only above this temperature.

The Bridgman relation permits one to calculate the thermal conductivity of a material from the measured

values of the Nernst and Ettingshausen coefficients. This was done for the samples used in our experiments and the results are shown in Fig. 3. These values for the thermal conductivity are seen to scatter around the straight line described by Eq. (2) on which the determination of the theoretical Ettingshausen coefficients was based.

## Statistical Potential for Actinide Metal Energy Band Calculations\*

GUY W. LEHMAN

*Atoms International, Canoga Park, California*

(Received October 9, 1959)

A simple analytic potential energy function,  $V$ , is developed from a Thomas-Fermi ion model for the actinide metals and is found to provide good agreement with wave functions derived from the Hartree self-consistent field approach by Ridley for the  $5f$ ,  $6d$ , and  $7s$  states of uranium. The estimated  $5f$ ,  $6d$ , and  $7s$  bandwidths are 1.1, 7.3, and 11.8 eV, respectively, in satisfactory agreement with those of Ridley.

Dirac's equations are solved for the  $5f$ ,  $6d$ , and  $7s$  states using this nonrelativistic potential energy function with the Wigner-Seitz boundary condition. The relativistic energy shift for the  $7s$  state is roughly 13 eV.

### I. INTRODUCTION

A ONE-ELECTRON statistical potential energy function is derived in this paper which is suitable for studying the electronic structure of the actinide metals, in particular, the cubic phases of thorium, uranium, and plutonium.

It was pointed out in a previous paper<sup>1</sup> that spin-orbit effects must be taken into account for an adequate description of the electronic structure of the actinide metals. A detailed approach was also presented which took spin-orbit coupling into account via an appropriate unitary transformation of the energy matrix,  $H_0$ , obtained by neglecting spin-orbit effects. The primary purpose of this paper is to derive a statistical potential energy function,  $V$ , which is currently being used to compute radial wave functions which are needed to determine the  $H_0$  matrix for gamma uranium using the 1937 version of Slater's augmented plane wave approach.<sup>2</sup>

Wave functions derived from this statistical potential approach are compared in Sec. III with the Hartree self-consistent (nonrelativistic) calculations carried out by Ridley for gamma uranium.<sup>3</sup>

Some numerical solutions of Dirac's equations using the statistical potential energy function derived in Sec. II are also presented in order to determine qualitative effects of relativistic forces on the  $5f$ ,  $6d$ , and  $7s$  orbitals in uranium. The numerical procedures for determining the relativistic as well as the nonrelativistic radial

wave functions used in this paper are outlined in an appendix.

### II. POTENTIAL FUNCTION

Each valence electron in the metallic actinides is considered to move in a potential field arising from three sources: (i) the nuclear charge for an ion whose atomic number is  $Z$  and the charge distribution due to the  $(1s)^2(2s)^2(2p)^6 \dots (5d)^{10}$  closed shell configuration of 78 electrons, (ii) the charge distribution due to the  $(6s)^2(6p)^6$  closed shell configuration of eight electrons, and (iii) the charge distribution due to the presence of the  $n_v - 1$  other valence electrons, where  $n_v$  is the total number of electrons outside closed shells. For thorium, uranium, and plutonium,  $n_v = 4, 6$ , and  $8$ , respectively.

#### A. Iron Core Potential Energy

In atomic units, the ion-core potential energy is given by

$$V_{\text{ion}}(r) = -\frac{2Z}{r} + 2 \int d\mathbf{r}' \frac{\rho_c(N, \mathbf{r}')}{|\mathbf{r} - \mathbf{r}'|}, \quad (1)$$

where  $\rho_c(N, \mathbf{r})$  is the electron density at the point  $\mathbf{r}$  of the  $N$  core electrons contained inside a sphere of radius  $r_c$ . If the  $6s$ ,  $6p$ , and valence electrons were absent, one could take  $\rho_c$  to be the usual Thomas-Fermi electron density,  $\rho_{TF}(N, \mathbf{r})$  associated with the ion under consideration here.<sup>4</sup> In the model used in this paper, it is assumed that  $\rho_c = \lambda^3 \rho_{TF}(N, \lambda \mathbf{r})$  is a good approximation

\* This work was supported by the U. S. Atomic Energy Commission.

<sup>1</sup> G. W. Lehman, Phys. Rev. **116**, 846 (1959).

<sup>2</sup> J. C. Slater, Phys. Rev. **51**, 846 (1937).

<sup>3</sup> E. Cicley Ridley, Proc. Roy. Soc. (London) **A247**, 199 (1958).

<sup>4</sup> For a discussion of the Thomas-Fermi ion model see P. Gombas, *Die Statistische Theorie des Atoms* (Springer-Verlag, Wein, 1949).